Supporting Information

Flower-like Fe_7S_8/Bi_2S_3 Superstructures with Improved Near-Infrared Absorption for Efficient Chemo-Photothermal Therapy

Qing Cao,[a] Xin Guo,[c] Wenlong Zhang,[a] Guoqiang Guan,[a] Xiaojuan Huang,[d] Shu-Ang He,[a] Mingdong Xu,[a] Rujia Zou,*[a] Xinwu Lu,*[c] and Junqing Hu*[a,b]

a. State Key Laboratory for Modification of Chemical Fibers and Polymer Materials, International Joint Laboratory for Advanced Fiber and Low-dimension Materials, College of Materials Science and Engineering, Donghua University, Shanghai 201620, P.R. China

b. College of Health Science and Environmental Engineering, Shenzhen Technology University, Shenzhen 518118, China

c. Department of Vascular Surgery, Shanghai Ninth People's Hospital, Shanghai JiaoTong University School of Medicine, Shanghai 200011, China

d. Department of Oral and Maxillofacial-Head Neck Oncology, Shanghai Ninth People's Hospital, College of Stomatology, Shanghai Jiao Tong University School of Medicine; National Clinical Research Center for Oral Diseases; Shanghai Key Laboratory of Stomatology & Shanghai Research Institute of Stomatology, Shanghai 200011, China

* Corresponding author

E-mail address: rjzou@dhu.edu.cn, luxinwu@shsmu.edu.cn, hu.junqing@dhu.edu.cn

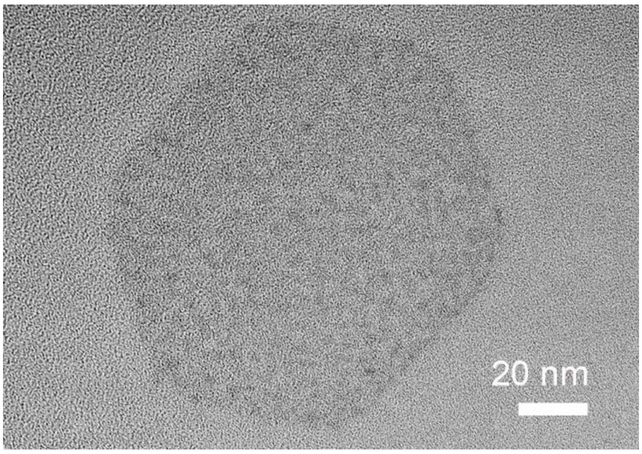

Fig. S1 TEM image of the Bi_2S_3 nanosheets.

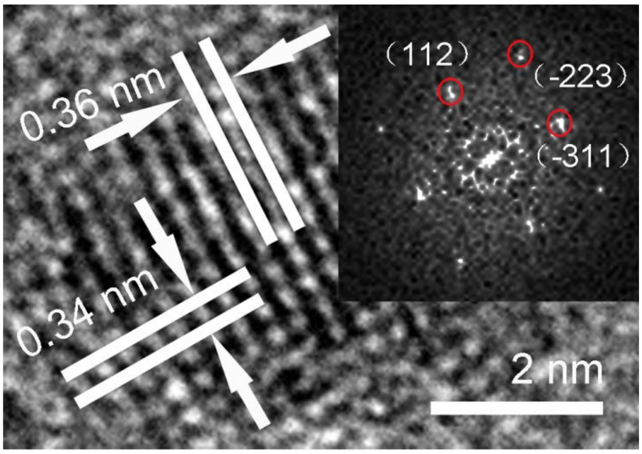

Fig. S2 HRTEM image of an Fe_7S_8 nanoparticle from an Fe_7S_8/Bi_2S_3 nanoflower (insertion: FFT pattern of this HRTEM image).

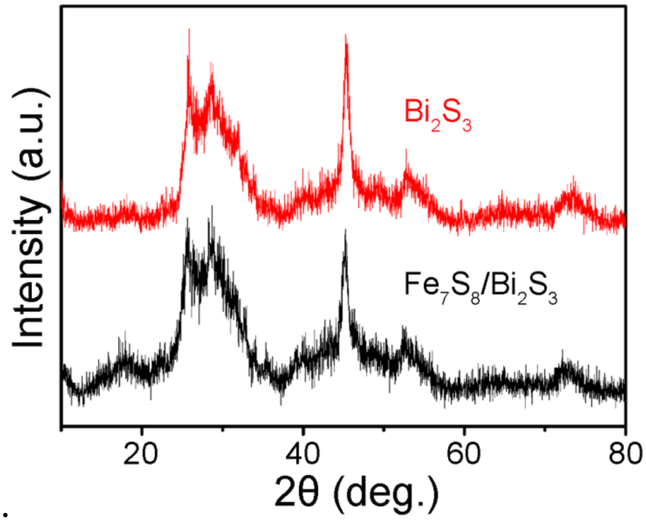

Fig. S3 XRD patterns of the Bi_2S_3 nanosheets (upper pattern) and Fe_7S_8/Bi_2S_3 nanoflowers (bottom pattern).

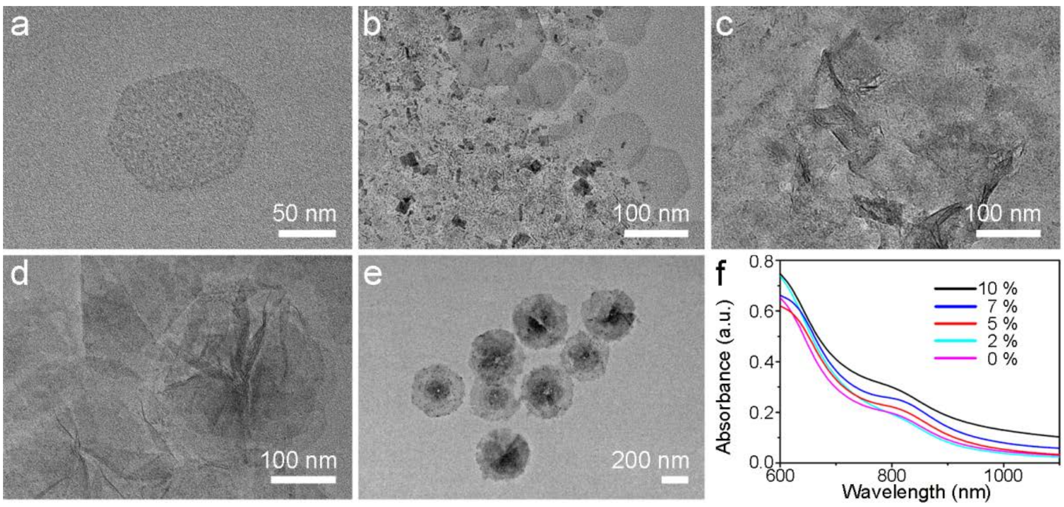

Fig. S4 (a-e) TEM images of samples with various percentages of Fe precursor: (a) 0% (Bi_2S_3 nanosheets), (b) 2%, (c) 5%, (d) 7%, and (e) 10% (Fe_7S_8/Bi_2S_3 nanoflowers). (f) UV-Vis-NIR absorption spectrum of the samples with the same concentration (25 μg/mL).

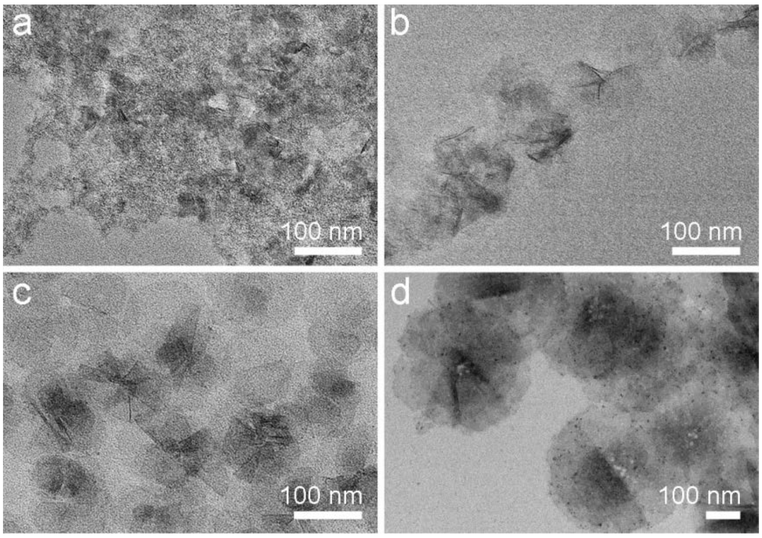

Fig. S5 TEM images of the products prepared at different reaction times: (a) 1 h, (b) 3 h, (c) 6 h, and (d) 12 h (final products).

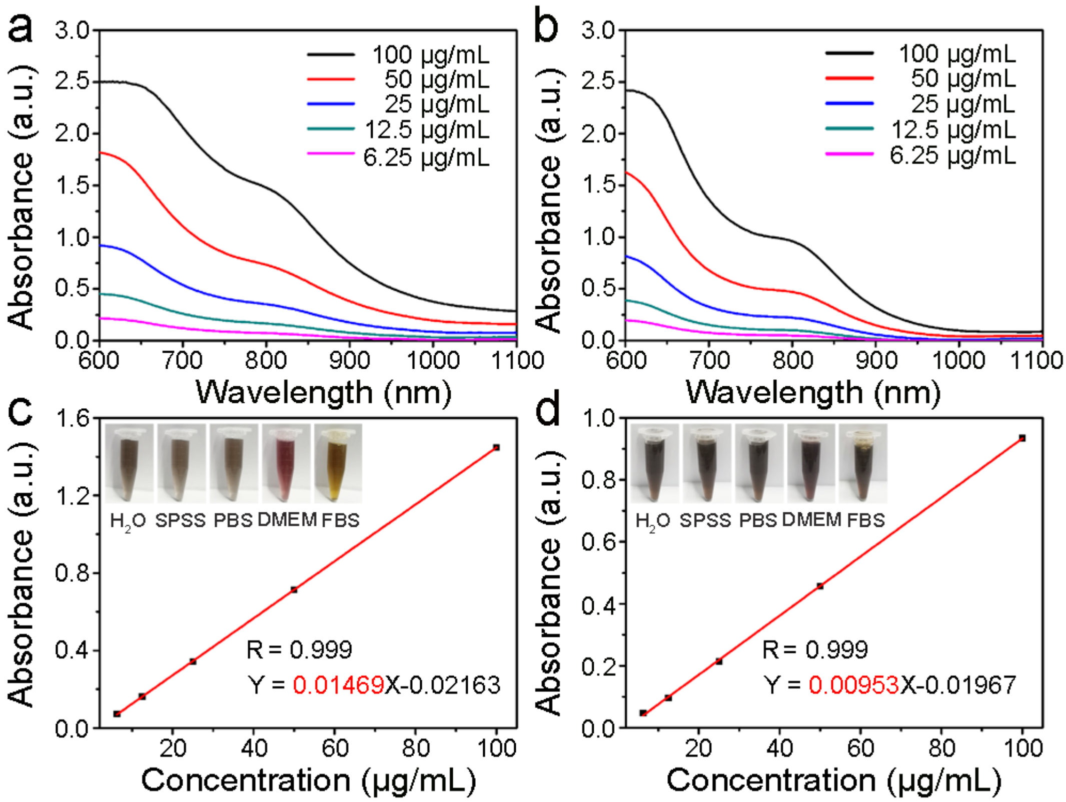

Fig. S6 (a, b) UV-Vis-NIR absorption spectra of the Fe_7S_8/Bi_2S_3 nanoflowers and Bi_2S_3 nanosheets' aqueous dispersions with different concentrations. (c, d) Linear fitting of the absorbance at 808 nm versus the Fe_7S_8/Bi_2S_3 and Bi_2S_3 concentration (insertion: the dispersion of the Fe_7S_8/Bi_2S_3 nanoflowers and Bi_2S_3 nanosheets in H_2O, SPSS, PBS, DMEM and FBS solutions, respectively).

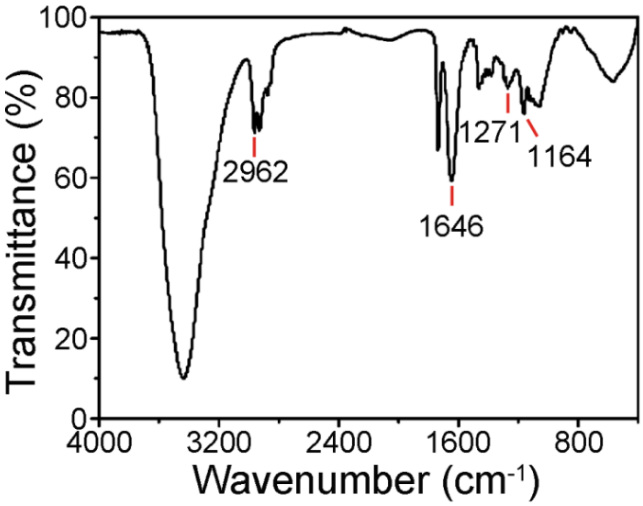

Fig. S7 FTIR spectroscopy of Fe_7S_8/Bi_2S_3 nanoflowers.

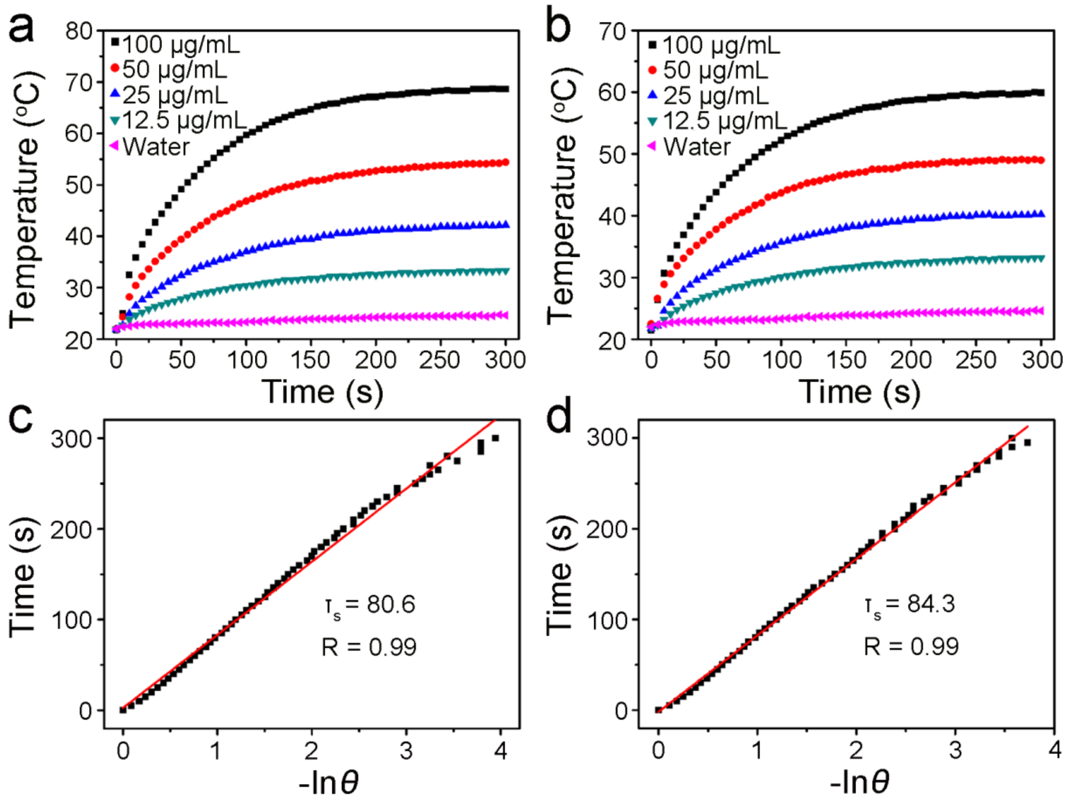

Fig. S8 (a, b) Temperature elevation of the Fe_7S_8/Bi_2S_3 nanoflowers and Bi_2S_3 nanosheets' aqueous dispersions with different concentrations under an 808 nm laser (1 W/cm^2) for 5 min. (c, d) Linear fitting of the cooling time data of the curves of the Fe_7S_8/Bi_2S_3 nanoflowers and Bi_2S_3 nanosheets from Fig. 2(c) vs. the responding negative natural logarithm of the temperature driving force (θ).

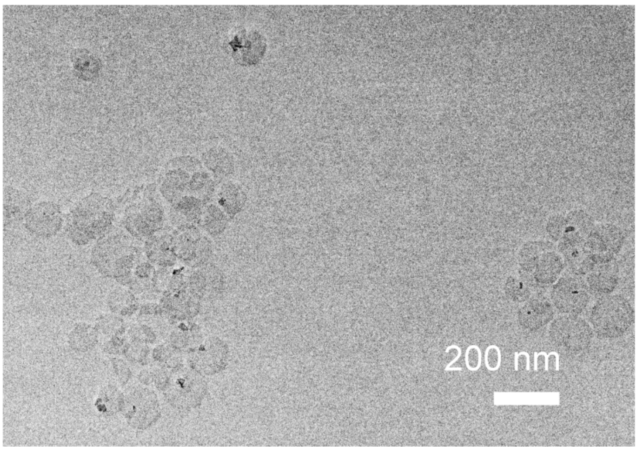

Fig. S9 TEM image of the Bi_2S_3 nanosheets' solution after laser irradiation.

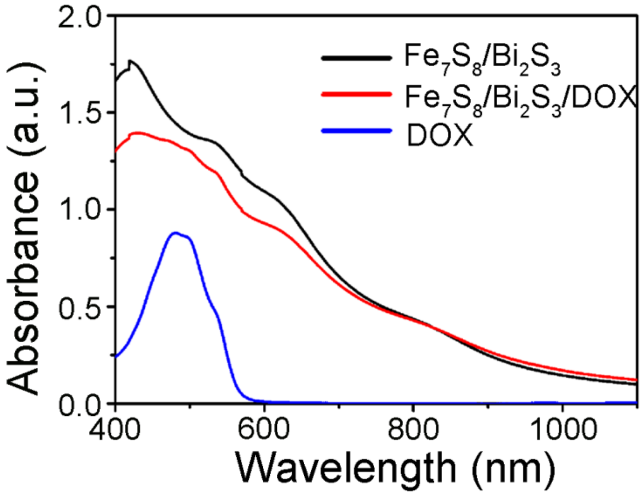

Fig. S10 UV-Vis-NIR spectra of the aqueous solutions of the DOX, Fe_7S_8/Bi_2S_3, and Fe_7S_8/Bi_2S_3/DOX.

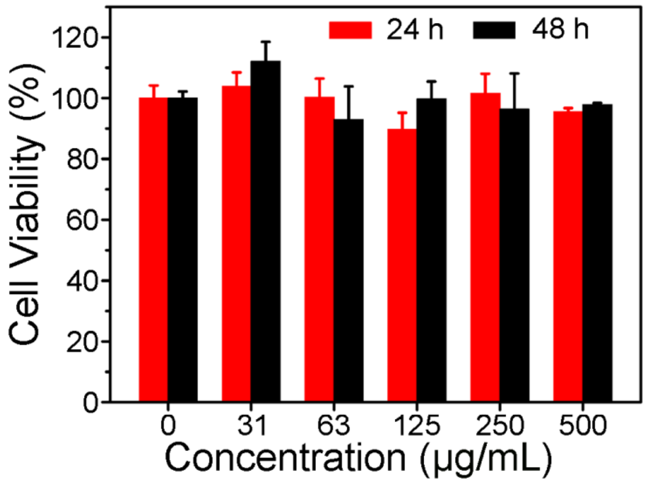

Fig. S11 Cell viability of 7721 cells after being treated with Fe_7S_8/Bi_2S_3 nanoflowers at various concentrations for 24 h and 48 h.

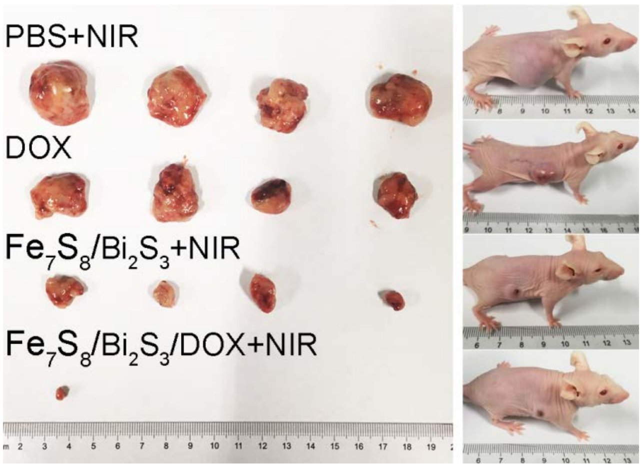

Fig. S12 Photos of the tumor-bearing mice and tumors after 20 days of treatments.

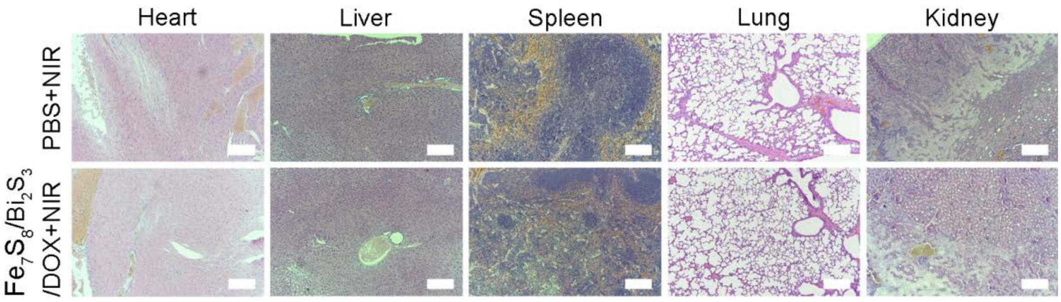

Fig. S13 H&E stained tissue sections of heart, liver, spleen, lung and kidney from the mice in PBS + laser and Fe_7S_8/Bi_2S_3/DOX + laser groups at 20th day after treatment. The scale bar is 145 μm.

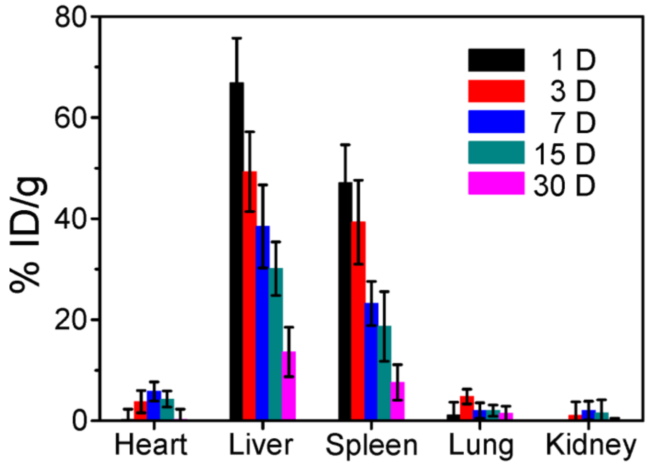

Fig. S14 The biodistribution of Bi in main organs including heart, liver, spleen, lung and kidney at 1st, 3rd, 7th, 15th, 30th day after i.v. injection with the Fe_7S_8/Bi_2S_3 nanoflowers (1 mg/mL, 200 μL).